Geophysical Research Letters

Supporting Information for

Persistent Long-Period Signals Recorded by an OBS Array in the Western-Central Pacific: Activity of Ambrym Volcano in Vanuatu

Yuki Kawano[1], Takehi Isse[1], Akiko Takeo[1], Hitoshi Kawakatsu[1], Daisuke Suetsugu[2], Hajime Shiobara[1], Hiroko Sugioka[3], Aki Ito[2], Yasushi Ishihara[2], Satoru Tanaka[2], Masayuki Obayashi[2], Takashi Tonegawa[2], and Junko Yoshimitsu[2]

[1]Earthquake Research Institute, The University of Tokyo, Tokyo, Japan

[2]Japan Agency for Marine-Earth Science and Technology, Kanagawa, Japan

[3]Graduate School of Science, Kobe University, Hyogo, Japan

Contents of this file

Introduction

This supporting information details (1) the location process of a local earthquake near the Ambrym island in Text S1, (2) the comparison of the power spectrogram for the 25 s signal and the 26 s signal in the Gulf of Guinea in Text S2, (3) the estimation of the instrument response for AMB1 and the evaluation of site amplification effects for AMB1 and SANVU in Text S3, (4) the comparison of the power spectrogram for the secondary microseism and the 25 s and 18 s signals in Text S4, and providing (5) a close-up spectrogram recorded at SANVU around the time of the 2015 eruption in Text S5.

Text S1. Locating a local earthquake near the Ambrym island

In order to assess the robustness of the inferred source location of the persistent sources in the Ambrym island (Figures 2b,c), we perform the same source location estimation process for a local earthquake near the Ambrym island (Mw 5.8, 167.14˚E, 16.29˚S, a depth of 13.5 km on April 30, 2016, 8:35:48.5UTC; the global CMT project). We define the time window for the earthquake starting at 1000 s before and ending at 2276.8 s after the origin time, and then cross-correlate the waveforms for each station pair. The estimated source location is 168.29˚E, 16.46˚S, showing about one-degree bias to the eastern direction. This bias may be caused by the lateral heterogeneity since the stations west of the estimated source location situate on the Australian Continent while the stations east of the estimated source location situate on the oceanic islands, resulting in the slower propagation on the western region compared to that of the eastern region. If we take this bias into account for the estimated source location of the 25 s signal, the location is 168.03˚E, 16.48˚S, which is close to the location of the station AMB1 (168.12˚E, 16.28˚S) in the Ambrym island.

Text S2. Comparison of the power spectrogram for the 25 s signal in the Vanuatu Arc and the 26 s signal in the Gulf of Guinea

Based on the comparison of the power spectrogram for the 25 s signal obtained from SANVU, on the Vanuatu Arc, and the 26 s signal obtained from MBO, a part of the GEOSCOPE network situated on the African Continent, we believe the possible contamination on the 25 s signal by the 26 s signal is small. The strength of the 25 s signal is more time-variable compared to that of the 26 s signal (Figures 3a and S1a). For example, the power of the 25 s signal is intensified at the end of March 2016 while the 26 s signal does not show any similar intensifications (Figure S1b). The result is consistent with Zeng and Ni (2014) which concluded that the two signal sources are independent. Considering that the estimated source in Vanuatu Arc is 18,500 km away from the previously estimated source in the Gulf of Guinea (Xia et al., 2013), the power of 26 s signal that should be observed at the Vanuatu Arc would be orders smaller than that of MBO. Besides, we believe that the antipodal focusing effect would not significantly affect the above discussion since the exact antipodal area of the Gulf of Guinea (Figure 5 in Shapiro et al., 2006) is deviated from our estimated source region (Figure 2a).

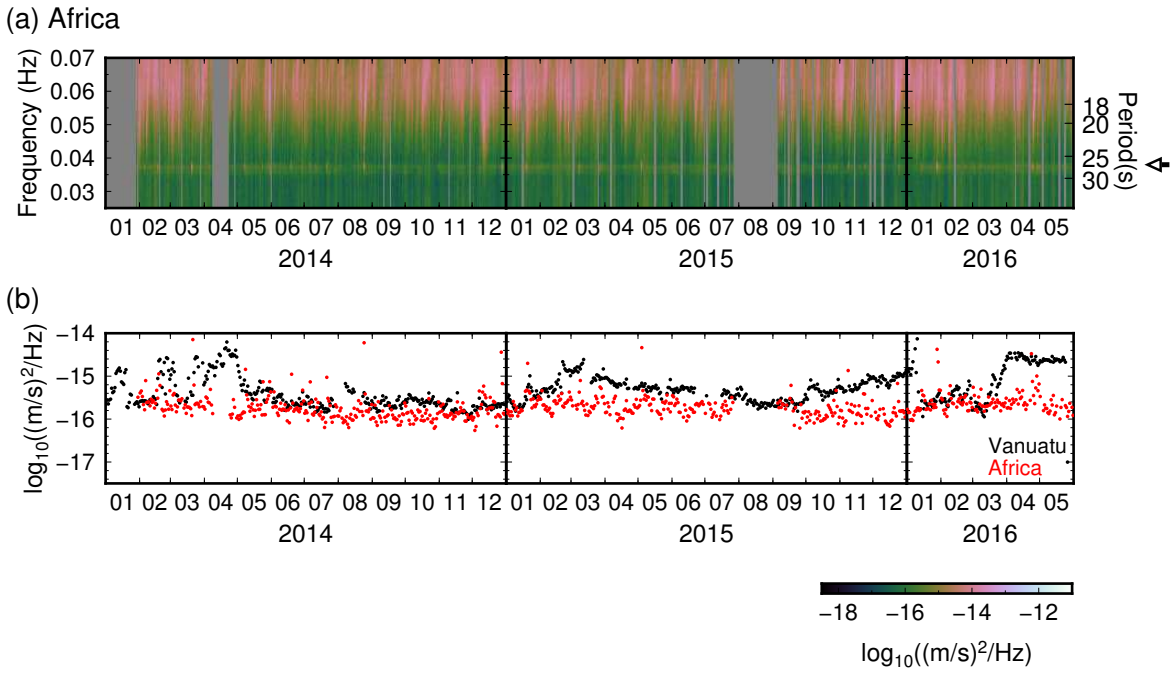

Figure S1. (a) Power spectrogram of MBO on the African Continent. The black arrow indicates the position of 0.038 Hz (26 s). (b) A comparison of power spectral densities of 25 s signal observed at SANVU on the Vanuatu Arc (averaged in a frequency range of 0.038–0.042 Hz) and 26 s signal observed at MBO (averaged in a frequency range of 0.037–0.039 Hz).

Text S3. Calibration of the instrument response for the station AMB1 using distant earthquakes

A comparison of the amplitude of distant earthquakes recorded at SANVU and AMB1 suggests that the instrument response of Guralp CMG-40T sensor at AMB1 provided by the IRIS DMC is likely to be incorrect. According to the IRIS DMC, the frequency response for AMB1 is flat to velocity from 1 Hz to 100 Hz. However, if we use the response to remove the instrument response, the amplitude of distant earthquakes, which are recorded at AMB1 and band-pass filtered between 0.01–0.02 Hz, is about two orders larger than that of SANVU located about 135 km away from AMB1 (Figure S2a). Since a CMG-40T sensor is provided with several options for the lower-corner frequency, we try to find a more reasonable frequency response by adjusting it: If we assume the lower-corner frequency to be 0.1 Hz (10 s) (Figure S2b and Table S1), the comparison of the amplitudes of distant earthquakes become reasonable (Figure S2a). Besides, the Fourier spectra of ambient noise recorded at AMB1 becomes more consistent with that of SANVU

at a frequency range of 0.1–0.3 Hz, where the secondary microseism exists (Figure S2c). Even using the revised instrument response, the power at AMB1 is still orders larger than that of SANVU at the frequency lower than 0.1 Hz because the instrumental noise is enhanced by the instrument response correction.

As the above response calibration is done at a frequency range of 0.01–0.02 Hz, it is possible that there exists some discrepancy between the real ground motion and response-corrected ground motion due to employed incorrect response correction and/or the physical site amplification/dis-amplification due to the difference in the local structure. We estimate this effect for a frequency range of 0.03–0.05 Hz, where our target signals reside at AMB1 and SANVU. Ten teleseismic earthquakes are selected based on the following criteria: (1) the epicentral distance is between 3,000–10,000 km, (2) the focal depth is shallower than 100 km, and (3) the magnitude is larger than or equal to 6.0. The selected seismograms are band-pass filtered between 0.03–0.05 Hz, and an 800 s-long seismogram that starts at a travel time for a group speed of 4.5 km/s, is prepared. For each earthquake-generated signal, a time-lag that maximizes the cross-correlation coefficient between AMB1 and SANVU is computed. The signals recorded by AMB1 and SANVU is shifted with the time-lag, and the amplitude ratio between two seismograms are computed. The average amplitude ratio is 0.33 that should be kept in mind whenever we discuss the amplitude for the two stations (Figures S3a,b).

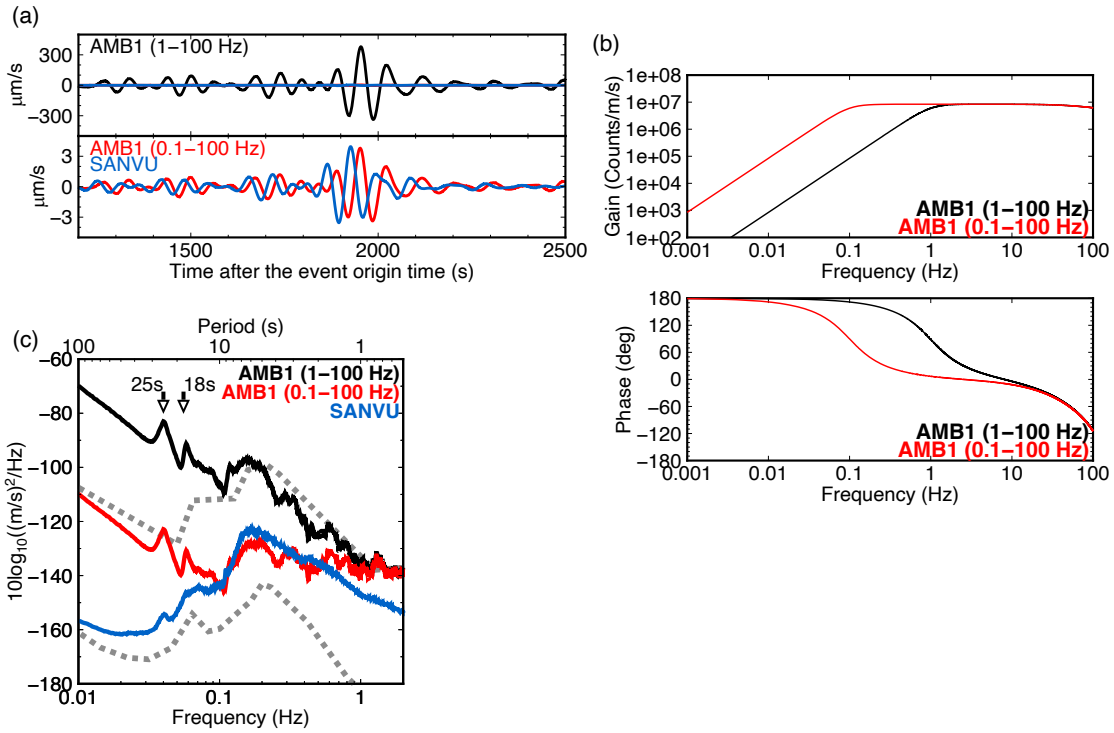

Figure S2. Comparison of instrument response corrected velocity seismograms recorded by AMB1 and SANVU using two different frequency responses for AMB1. (a) Vertical component records of a distant earthquake (Mw 7.0 in the Aleutian Islands, August 30, 2013 at an epicentral distance of 61.9˚) band-pass filtered between 0.01–0.02 Hz. The black and red seismograms represent records from AMB1 assuming the 1–100 Hz response and 0.1–100 Hz velocity flat responses, respectively. The blue seismograms represent the same waveform for SANVU. (b) The response curves of 0.1–100 Hz (red) and 1–100 Hz (black) velocity flat responses: gain (top) and phase (bottom) with total sensitivity referenced at 5 Hz, where the total sensitivity of AMB1 reported by IRIS (the 1-100 Hz response) is used for both cases. (c) Power-spectral density of ambient noise for SANVU (blue) and AMB1 with 1–100 Hz response (black) and 0.1–100 Hz response (red). The gray lines show New Low and High Noise Models (Peterson, 1993).

Table S1

Poles and Zeros (in rad/s) for 0.1-100 Hz

Poles 6	Zeros 2
-0.44422+0.44422i	0.00000
-0.44422-0.44422i	0.00000
-391.96+850.69i	
-391.96-850.69i	
-471.24	
-2199.1	

Note. Normalization factor at 5 Hz : 9.10601e+11

Table S1. Poles and zeros of the 0.1–100 Hz velocity flat response for AMB1.

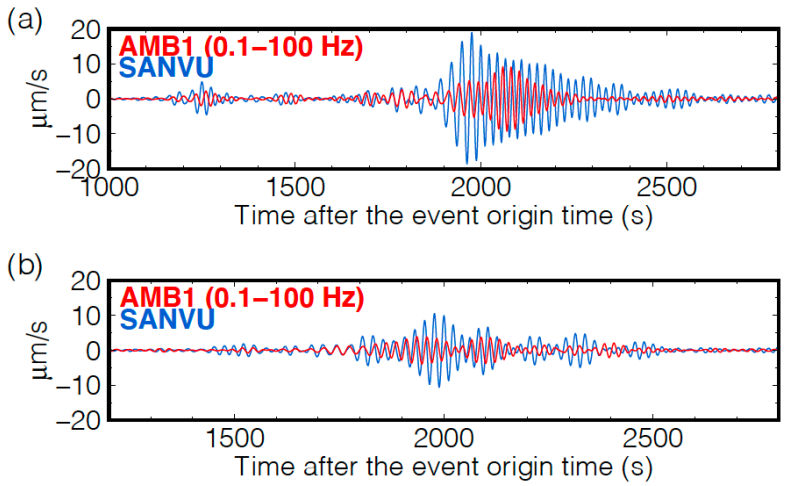

Figure S3. Comparison of earthquake-generated signals recorded at AMB1 (red) and SANVU (blue). Seismograms are band-pass filtered between 0.03–0.05 Hz. (a) for the same earthquake in Figure S2a, (b) for an Mw 6.6 earthquake (in South of Java Islands, June 13, 2013, 59.4˚).

Text S4. Comparison of the secondary microseism with the 25 s and 18 s signals

Figure S4 shows the power spectrogram of AMB1 at the frequency range of 0.025–0.25 Hz. The time variation of power spectral densities for the 25 s and 18 s signals are not consistent with that of the secondary microseism (5–10 s). For example, the power at 0.2 Hz during the middle of July is higher than the rest of the days in July, whereas the power of the 25 s and 18 s signals in July does not show associated time variation.

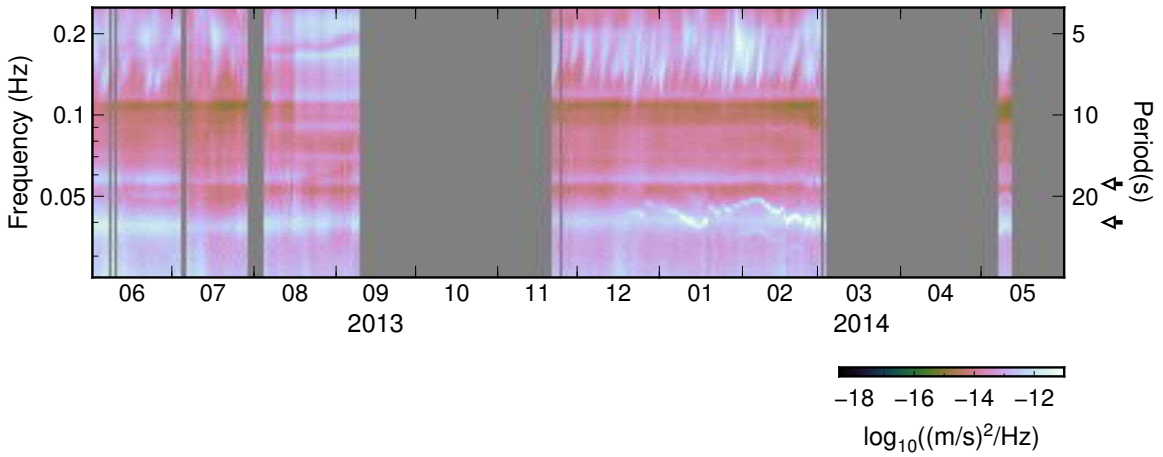

Figure S4. Power spectrogram (0.025–0.25 Hz) of vertical component recorded at AMB1. Black arrows indicate positions of 25 s and 18 s.

Text S5. Intensification of the 25 s signal associated with the 2015 eruption

A power spectrogram of the vertical component seismogram recorded at SANVU shows that the intensification of the 25 s signal power corresponds the minor eruption on February 20, 2015 (Hamling and Kilgour, 2020). The 25 s signal power gets stronger and the dominant period becomes longer after the eruption (at about 30 hours after the Mw 6.4 earthquake). The 18 s signal seems to hide behind the primary microseism that are dominant at around 15 s. The spectrogram is computed using 409.6 s-long time window with a 50 % overlap (Figure S5).

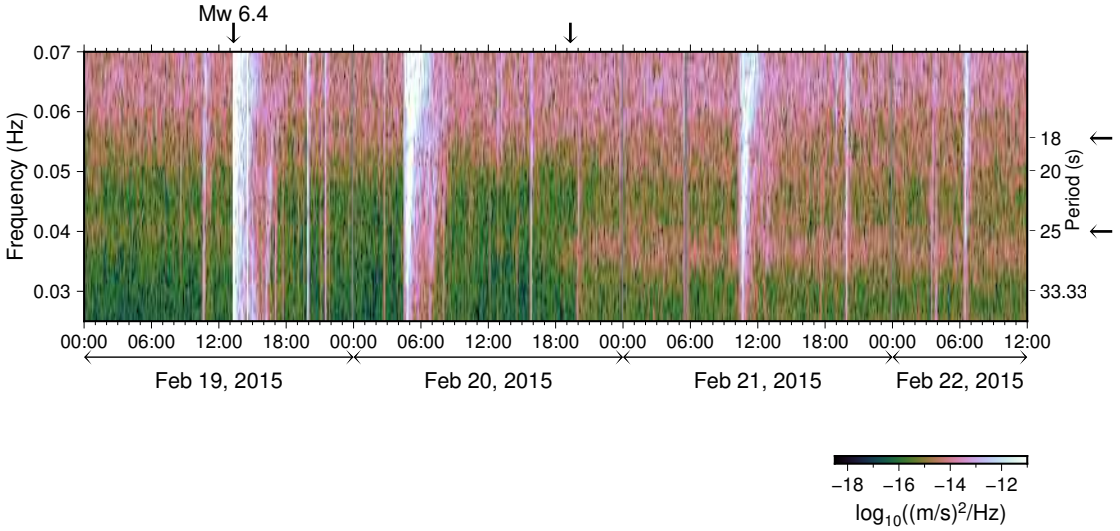

Figure S5. Power spectrogram of vertical component recorded at SANVU around the time of the 2015 eruption (closed-up of Figure 3a). Black arrows on the top represent the timing of the Mw 6.4 local earthquake and the time 30 hours after the earthquake occurrence that corresponds the onset of the eruption according to Hamling and Kilgour (2020). Black arrows on the right axis represent the position of 18 s and 25 s.